Topic	Earthquake location at teleseismic distances by hand from 3-component records
Author	Peter Bormann, and Kurt Wylegalla (formerly GeoForschungsZentrum Potsdam, Telegrafenberg, D-14473 Potsdam, Germany); E-mail: pb65@gmx.net
Version	October 2002

1 Aim

The exercise aims at making you familiar with the basic concept of locating seismic events by means of teleseismic records from single 3-component stations. Often the results are comparably good or even better than for uncalibrated single seismic arrays.

The exercise uses teleseismic events only although the procedure outlined below is the same for local seismic events. In the latter case local travel-time curves as in Exercise EX 11.1 have to be used for phase identification and distance determination. Note however that azimuth determinations for local events are less reliable when short-period records are used. They are much more influenced by local heterogeneities in the crust than teleseismic long-period or broadband records. Accordingly, particle motion might deviate significantly from linear polarization (see Fig. 2.6) and the azimuth of wave approach for local events sometimes deviates more than 20° (+ 180°) from the backazimuth AZI towards the source (Fig. 11.23).

2 Data

The following data are used in the exercise:

- two 3-component earthquake records: a) Kirnos BB-displacement seismogram (Figure 2) and b) long-period (WWSSN-LP) seismogram (Figure 3);
- differential body-wave travel-time curve (with respect to the P-wave first arrival) for the distance range 0° < D ≤ 100° (Figure 4);
- IASP91 table of travel-time differences pP-P and sP-P, respectively, as a function of epicentral distance D (in degree) and source depth h (in km) (see Table 1);
- global map of epicenter distribution with isolines of epicentral distance D (in °) and principal directions of backazimuth AZI from station CLL (Germany).

3 Procedure

3.1 Estimation of epicentral distance D and depth h

- Identification of first as well as later secondary arrivals from teleseismic events in broadband or long-period filtered records. At least P and S have to be identified. P is the first arrival (up to about 100°) and for teleseismic events strongest in the vertical component. S is the first arriving shear wave up to about 83° and has its largest amplitudes in horizontal components. For larger distances SKS becomes the first arriving shear wave (see Figure 4). Misinterpreting it as S might result in significant underestimation of the epicentral distance.

- Determination of epicentral distance D by using the travel-time difference t(S-P) according to travel-time tables (e.g., IASPEI 1991; Kennett 1991) or by fitting best a set of differential travel-time curves as in Figure 4 with the identified phases in the record. Note that the records and the t-D-curves must have the same time scale. In the distance range 20° < D < 85° the following **rule-of-thumb** allows to determine D with an error < 3°: $\mathbf{D\ [°] = [t(S\text{-}P)_{[min]} - 2] \times 10}$.

- Note, that the travel-time difference t(S-P) but also the time difference between P or PKP (beyond 105°) with other secondary phases is influenced by the source depth h. Unrecognized significant source depth might result in underestimating D by several degrees. Accordingly, it is important to assess from the outset whether an event was deep or shallow (i.e., probably within the crust).

- For a first rough discrimination between deep and shallow earthquakes one should compare the amplitudes of body waves with that of (dispersed !) surface waves. If the latter are well developed and significantly larger in amplitude than the earlier body waves, then the event can be considered a crustal earthquake. Since for shallow events it is difficult to identify any depth phases, which follow closely to the P or S onset, one may use travel-time curves or tables for surface focus (h = 0 km) or "normal depth" events (h = 33 km).

- In case of relatively weak or absent surface waves one should look for depth phases! Examples for depth phases are given in DS 11.2, Figures 7b, 9a, 16b and in DS 11.3 Figures 3b-d and 5a. See also the discussion in section 11.5.4. If depth phases such as pP and/or sP have been identified h can be calculated, when the epicentral distance is roughly known, by using differential travel-time pP-P or sP-P (see Table 1). If no such tables are available, one may also use another rule-of-thumb for a rough estimate, namely **h [km] ≈ 0.5 t(pP-P) [s] × 7** (for h < 100 km),…**× 8** (for h = 100 – 300 km) or…**× 9** (for h > 300 km).

3.2 Estimation of backazimuth AZI

- Identify the proper direction of P-wave first motion in the three components Z, N, E. Make sure by exact time correlation that you really compare the same first half cycles in all three records! This is particularly important, if in one of the horizontal components the first onset is very weak or near to zero. Then one might be misled and associate the stronger amplitude of a later half cycle with the first motion in the other components and get a wrong backazimuth.
- Determine the direction of particle motion from the amplitudes of first motions in the horizontal component records according to the formula $\mathbf{AZI = arc\ tan\ (A_E/A_N)}$. If seismograph components have been calibrated properly and avail of identical frequency responses (which is the case in these exercises) then one just calculates the ratio between measured trace amplitudes. However, as demonstrated in Figure 1, this direction may either show **towards the epicenter,** in case the first motion in Z is down (-, dilatational; see blue record traces), or away from the epicenter if the first motion in Z is up (+, compressional; see red record trace). In the latter case, the backazimuth to the epicenter is AZI + 180°.

  - If this 180° ambiguity has been resolved, one may also calculate the azimuth from horizontal component records of either later cycles of P with larger amplitudes or even by using the amplitude ratio in E/N from other later phases which are polarized in the vertical propagation plane such as PP, SKS, SP etc.

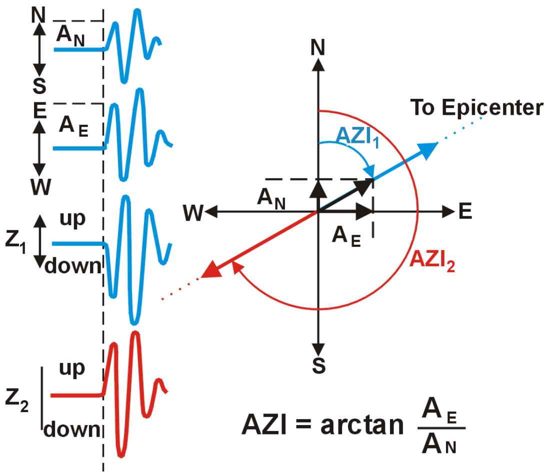

Figure 1 Principle of (back)azimuth determination from P-wave first-motion amplitudes.

3.3 Event location using the estimated epicentral distance D and backazimuth AZI

- You may use a sufficiently large globe (diameter about 0.5 to 1 m), mark there the position of your station and then use a bendable ruler with the same scale in degree as your globe and an azimuth dial to find your event location on the globe.
- Another possibility is that you get a regional (Figure 5) or global map projection (Figure 6) which shows isolines of equal azimuth and distance from your station. Such maps can nowadays easily be calculated and plotted for any station with known co-ordinates together with the the seismicity pattern.l

4 Tasks

4.1 Event No. 1 (record Figure 2)

4.1.1 Assess, whether the source was shallow (< 70 km) or deep (Look for surface waves!)

- Shallow source?
- Deep source?

4.1.2 Look for possible depth phases. Are there any clear depth phases?

- Yes?
- No?
- Comments on the possible depth range of the EQ if you suspect pP and/or sP to arrive in the complex wave group after P?

4.1.3 If you do not find any clear depth phases use the differential travel-time curve in Figure 4 (which is for surface foci), and try to identify the principal phases in the vertical and horizontal component record.

- Which phases have you identified?
- Give reasons for your interpretation?

4.1.4 Match your differential travel-time curve with your identified phases. Read the distance D for your best fit and write it down:

- D = ……°

4.1.5 Determine the backazimuth AZI from the amplitude ratio A_E/A_N using the equation given in Figure 1 and taking into account the related explanations given in 3.2.

- AZI =……°

4.1.6 Locate the epicenter on the map given in Figure 5.

- Source region?
- Discussion?

4.2. Event No. 2 (record Figure 3)

4.2.1 Assess, whether the event was shallow (< 70 km) or deep by looking for possible surface waves in the full record, which is inserted at strongly compressed time scale.

- Shallow event?
- Deep event?

4.2.2 Look for possible depth phases. Are there any clear depth phases?

- Yes?
- No?
- Comments?

4.2.3 Measure the time difference (in min) between the P-wave first arrival and the five marked onsets of stronger secondary wave arrivals in the records. Note that 1 cm = 1 min. Write down the time differences Xi-P (in min) in the order of their appearance.

- X1-P = , X2-P = , X3-P = , X4-P = , X5-P = ?

4.2.4 In order to match these travel-time differences with the differential travel-time curve presented in Figure 4 (time scale: 1.5 cm = 1 min!), multiply these differences with 1.5. Mark the respective distances to the P-wave onset on the edge of a sheet of paper, place the P-wave onset mark on the ordinate (distance scale) and try to match the later onset marks with the differential travel-time curves given in Figure 4. Read the distance D (in °) for your best match of travel-time curves with as many as possible of your onset marks and identify the phases related to the later onsets (give phase names):

- D (CLL) = ...°,
- X1 = , X2 = , X3 = , X4 = , X5 =
- Comments, which support your phase interpretations ?

4.2.5 Determine the backazimuth AZI as in task 4.1.5.

- AZI (CLL) = ...°

4.2.6 Locate the event as in task 4.1.6 by using Figure 6

- Name of source region/country?

5 Solutions

Note: Your estimates for the travel-time differences should be within about 0.2 min, for D within 2° and for the backazimuth AZI within about 5° of the solutions given below.

Event No. 1:

4.1.1 The earthquake is deeper than 70 km because no surface waves have been recorded.

4.1.2 No clear depth phases recognizable. They might however arrive within the complex wave group, which follows within about 40 s after the P onset. The ISC gives a hypocenter depth h = 111 km and an epicentral distance D = 20.24° for station MOX. According to Table 1 pP should then arrive about 21 s and sP about 35 s after P. Therefore, the first two sharp recognizable onsets after P on the Z component record are most likely the depth phases pP and sP, not PP and PPP as shown in the simplified J-B-differential travel-time curve of Figure 4. According to more recent travel-time models such as IASP91 (see DS 2.1) PP and PPP proper appear only for $D \geq 30°$.

4.1.3 You should have identified at least P (and probably PP and PPP or depth phases) on the Z component, the S wave as the largest onset on the E component, and SS (with longer period than S) on the N component.

4.1.4 **D ≈ 20°** (the ISC gives for station MOX D = 20.24°)

4.1.5 **AZI ≈ 125°** (from P-wave first motion amplitudes)
AZI ≈ 132° (from P-wave maximum peak-to-trough amplitudes).

4.1.6 Using our results from 4.1.5 and the map in Figure 5 we locate the earthquake in the coastal area of **southern Turkey.** ISC gives the coordinated 36.46 °N and 31.72 °E. This is near the coast of southern Turkey. Locating a sub-crustal earthquake there makes sense, because the African Plate is sub-ducted underneath southern Turkey.

Event No. 2:

4.2.1 Shallow earthquake with strong surface waves in the insert, with A_{max} after about 37 min.

4.2.2 No depth phases recognizable in the LP records (NEIC reported for this earthquake a hypocenter depth of h = 19 km).

4.2.3 X1-P ≈ 3.65 min, X2-P ≈ 10.5 min, X3-P ≈ 11 min, X4-P ≈ 12.2 min, X5-P ≈ 17 min

4.2.4
- **D (CLL) ≈ 93°** ± 1° for the best match of the travel-time differences given under 4.2.3 with the with the travel-time curve shown in Figure 4. NEIC-PDE gives for station CLL 92.6°.
- The identified phases are: X1 = PP, X2 = SKS, X3 = S, X4 = PS/SP, X5 = SS
- Both SKS and PS are strongest in the horizontal component E where also P has its largest horizontal amplitude. At about the time of PS in N there appears also in Z a clear energy arrival (SP!). S arrives later than SKS and is strong in the N component only.

4.2.5 **AZI(CLL**) ≈ 270° (first motion in N not visible! Recognizable P-wave first motion in the N component begins more than 6 s later than in the Z component!). NEIC-PDE gives for CLL AZI = 272.3°.

4.2.6 Using the map in Figure 6 for station CLL gives the **source area** as **Ecuador.** NEIC-PDE gives as epicenter coordinates 0.59°S and 80.39°W, i.e., near coast of Ecuador. This is very close to our location.

Figure 2 (next page) 3-component record of a Kirnos BB-displacement seismograph at station MOX, Germany. The time scale is 15 mm/minute. All seismograph components have properly been calibrated and identical magnification.

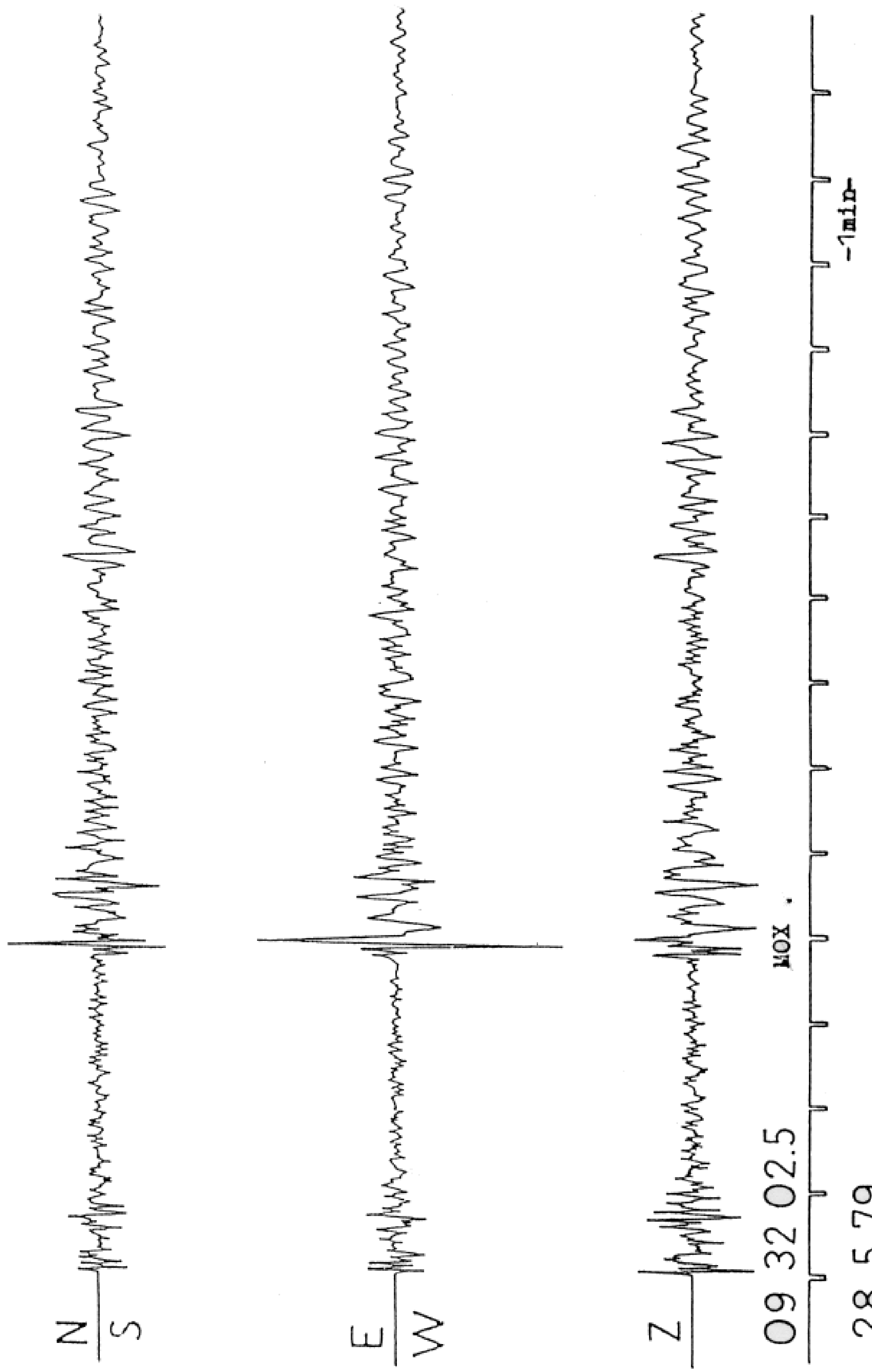

Figure 2

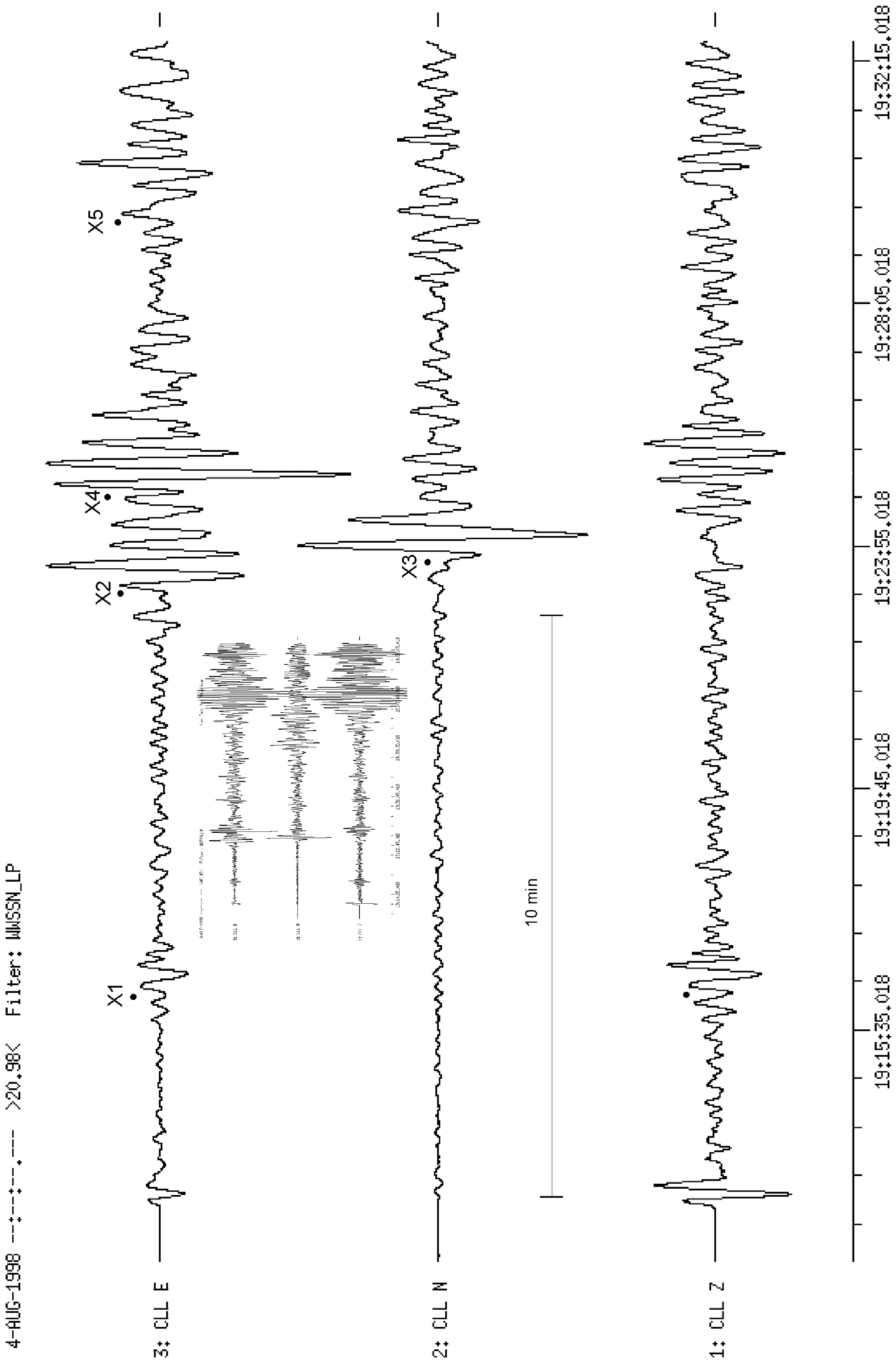

Figure 3 Long-period 3-component record section (WWSSN-LP simulation) of station CLL, Germany. **Time scale: 1 cm = 1 min**. Insert: Complete event record at compressed time scale.

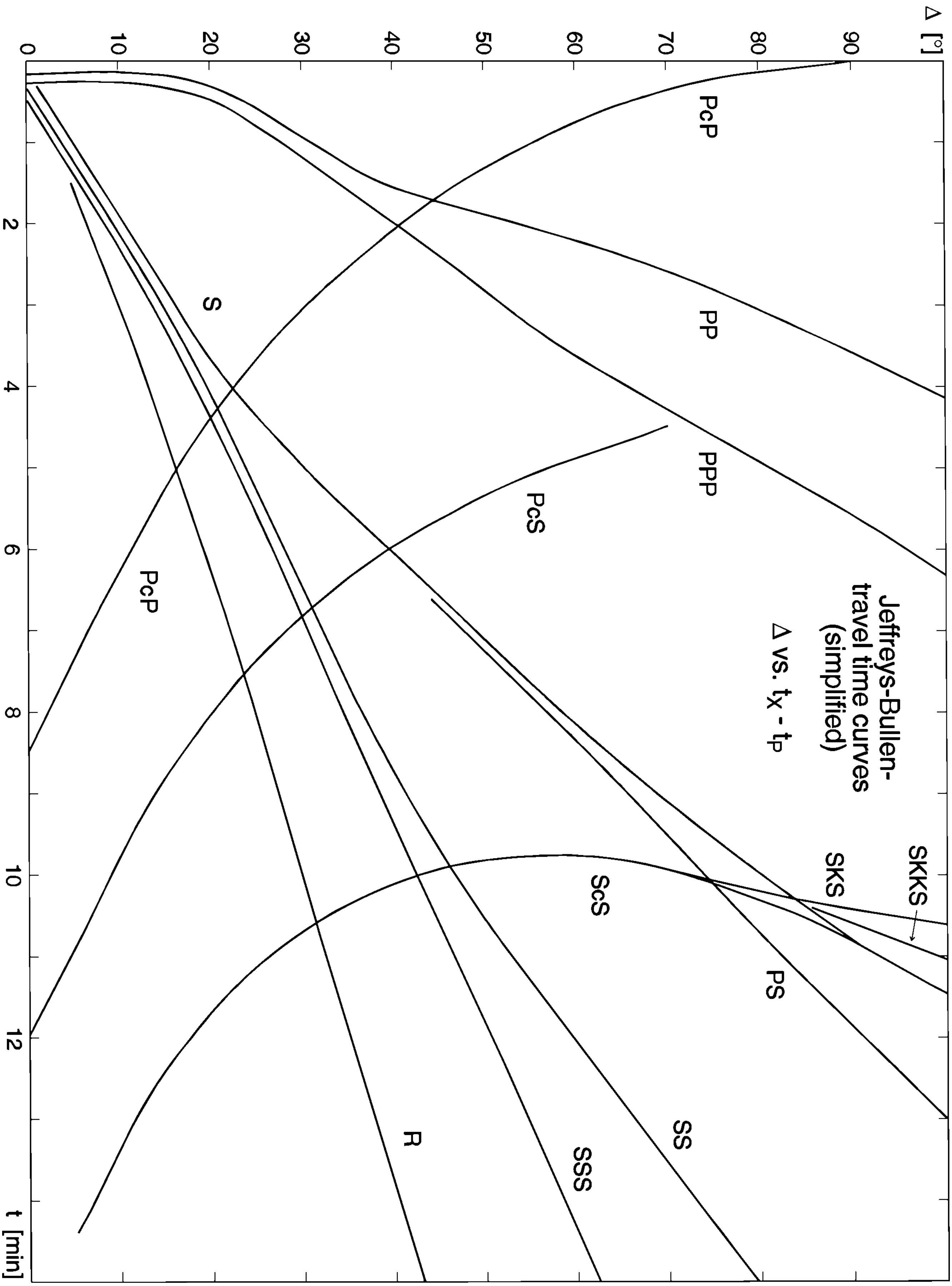

Figure 4 Simplified Jeffreys-Bullen differential travel-time curve in the distance range 0° < D ≤ 100°. Time scale: 15 mm = 1 min.

Figure 5 Regional map for Europe and the Mediterranean with earthquake epicenters and isolines of D and AZI with respect to station MOX.

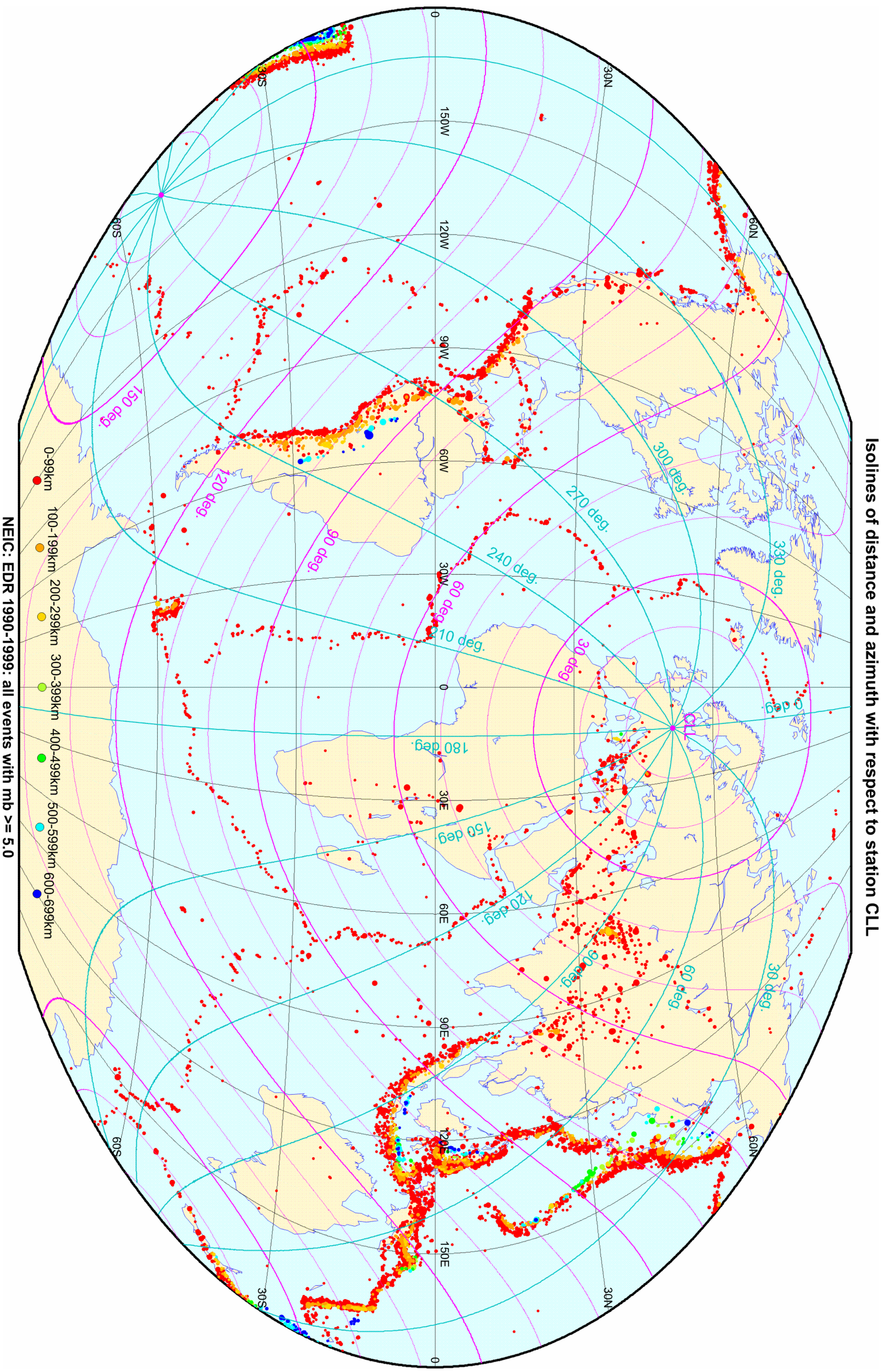

Figure 6 World map with epicenters and isolines of D and AZI with respect to station CLL.

Table 1 Travel-time differences pP-P and sP-P as a function of distance D and depth h according to the IASP91 travel-time tables (Kennett, 1991).

pP-P	Depth of source [km]										
Δ	15.	35.	50.	100.	150.	200.	250.	300.	400.	500.	600.	700.
	s	s	s	s	s	s	s	s	s	s	s	s
2	3.6	7.5										
4	3.6	7.5										
6	3.6	7.5										
8	3.6	7.5										
10	3.6	7.6										
12	3.6	7.6	7.9									
14	3.6	7.6	8.0									
16	3.8	8.1	9.3	20.1	26.2							
18	4.0	8.5	10.1	16.2	25.9	32.6	38.8					
20	4.3	9.2	11.5	19.0	25.6	33.2	39.6	45.4				
22	4.3	9.3	11.7	19.4	26.9	34.4	41.7	48.4	59.9			
24	4.5	10.0	12.7	21.4	29.8	37.8	45.3	52.2	64.1	82.7		
26	4.6	10.0	12.8	22.1	31.3	40.2	48.7	55.8	68.2	83.4	93.4	
28	4.6	10.0	12.9	22.3	31.5	40.5	49.1	57.2	72.2	84.3	94.4	
30	4.6	10.1	12.9	22.4	31.7	40.8	49.4	57.7	72.9	85.2	95.6	
32	4.6	10.1	13.0	22.5	31.9	41.0	49.8	58.1	73.5	86.1	96.8	
34	4.6	10.1	13.0	22.6	32.1	41.3	50.1	58.5	74.1	87.0	98.1	
36	4.6	10.2	13.1	22.8	32.3	41.6	50.5	59.1	74.9	88.0	99.4	
38	4.6	10.2	13.1	22.9	32.6	42.0	51.0	59.6	75.6	89.1	100.8	109.7
40	4.7	10.2	13.2	23.1	32.8	42.3	51.4	60.2	76.5	90.2	102.2	111.6
42	4.7	10.3	13.3	23.2	33.1	42.7	51.9	60.8	77.3	91.3	103.7	113.5
44	4.7	10.3	13.4	23.4	33.4	43.0	52.4	61.3	78.1	92.4	105.1	115.4
46	4.7	10.4	13.4	23.6	33.6	43.4	52.8	61.9	78.9	93.5	106.6	117.3
48	4.7	10.4	13.5	23.7	33.9	43.7	53.3	62.5	79.7	94.6	108.0	119.1
50	4.7	10.5	13.6	23.9	34.1	44.1	53.7	63.0	80.5	95.6	109.3	120.9
52	4.8	10.5	13.6	24.0	34.4	44.4	54.2	63.5	81.3	96.7	110.7	122.7
54	4.8	10.5	13.7	24.2	34.6	44.8	54.6	64.1	82.0	97.7	112.0	124.3
56	4.8	10.6	13.8	24.3	34.8	45.1	55.0	64.6	82.7	98.6	113.2	125.9
58	4.8	10.6	13.8	24.5	35.1	45.4	55.4	65.1	83.4	99.6	114.5	127.5
60	4.8	10.7	13.9	24.6	35.3	45.7	55.8	65.6	84.1	100.5	115.6	129.0
62	4.8	10.7	13.9	24.8	35.5	46.0	56.2	66.0	84.8	101.4	116.8	130.4
64	4.9	10.7	14.0	24.9	35.7	46.3	56.5	66.5	85.4	102.2	117.9	131.8
66	4.9	10.8	14.1	25.0	35.9	46.5	56.9	66.9	86.0	103.1	119.0	133.2
68	4.9	10.8	14.1	25.1	36.1	46.8	57.2	67.4	86.6	103.9	120.0	134.5
70	4.9	10.8	14.2	25.3	36.3	47.1	57.6	67.8	87.2	104.7	121.0	135.8
72	4.9	10.9	14.2	25.4	36.5	47.3	57.9	68.2	87.8	105.4	122.0	137.0
74	4.9	10.9	14.3	25.5	36.7	47.6	58.2	68.6	88.4	106.2	122.9	138.2
76	4.9	10.9	14.3	25.6	36.8	47.8	58.6	69.0	88.9	106.9	123.9	139.3
78	4.9	11.0	14.4	25.7	37.0	48.1	58.9	69.3	89.4	107.6	124.8	140.5
80	5.0	11.0	14.4	25.8	37.2	48.3	59.2	69.7	90.0	108.3	125.7	141.5
82	5.0	11.0	14.5	25.9	37.4	48.5	59.5	70.1	90.5	109.0	126.5	142.6
84	5.0	11.1	14.5	26.1	37.5	48.8	59.8	70.4	91.0	109.7	127.4	143.7
86	5.0	11.1	14.6	26.1	37.7	49.0	60.0	70.8	91.4	110.3	128.2	144.7
88	5.0	11.1	14.6	26.3	37.9	49.2	60.4	71.2	92.0	111.0	129.0	145.6
90	5.0	11.1	14.6	26.3	37.9	49.3	60.5	71.4	92.3	111.4	129.5	146.3
92	5.0	11.1	14.7	26.3	38.0	49.4	60.6	71.5	92.4	111.6	129.8	146.6
94	5.0	11.1	14.7	26.4	38.0	49.5	60.6	71.5	92.5	111.7	130.0	146.9
96	5.0	11.2	14.7	26.4	38.1	49.5	60.7	71.6	92.7	111.9	130.2	147.2
98	5.0	11.2	14.7	26.4	38.1	49.6	60.8	71.8	92.8	112.1	130.5	147.5
100	5.0	11.2	14.7	26.5	38.1	49.6	60.9	71.8	92.9	112.2	130.6	147.6

sP-P	Depth of source [km]										
Δ	15.	35.	50.	100.	150.	200.	250.	300.	400.	500.	600.	700.
	s	s	s	s	s	s	s	s	s	s	s	s
2	5.9	12.7	15.4	22.8	27.0	35.7						
4	5.9	12.7	15.5	24.4	32.4	40.0	46.9	53.1	63.7			
6	5.9	12.7	15.6	24.8	33.5	42.0	50.1	57.5	70.6	81.2	89.2	
8	5.9	12.7	15.6	25.0	34.3	43.5	52.4	60.8	75.8	88.6	98.5	106.0
10	5.9	12.7	15.7	25.3	35.1	45.0	54.6	63.7	80.6	95.1	106.6	115.9
12	5.9	12.8	15.7	25.7	36.3	46.7	57.0	66.7	86.0	101.4	114.0	125.3
14	5.9	12.8	15.8	26.8	38.0	49.0	59.8	70.5	91.4	107.7	121.3	134.6
16	6.0	13.1	16.7	28.6	40.4	52.4	64.4	75.9	97.2	114.1	130.3	143.9
18	6.1	13.4	17.2	30.5	43.6	56.5	69.0	80.9	103.0	121.7	139.3	153.3
20	6.3	13.9	18.1	31.9	45.5	58.9	72.0	84.6	108.5	129.6	148.2	162.8
22	6.4	14.0	18.2	32.2	46.0	59.9	73.8	87.3	113.0	135.2	155.5	171.4
24	6.6	14.5	19.0	34.0	48.6	63.0	77.1	90.7	116.5	139.1	159.6	177.1
26	6.6	14.5	19.0	34.1	49.0	63.7	78.1	92.1	118.8	142.4	163.5	181.3
28	6.6	14.6	19.1	34.2	49.2	64.0	78.5	92.5	119.3	143.0	164.9	184.0
30	6.6	14.6	19.1	34.3	49.3	64.1	78.7	92.8	119.7	143.6	165.7	185.1
32	6.6	14.6	19.2	34.4	49.4	64.3	78.9	93.1	120.2	144.2	166.5	186.2
34	6.6	14.6	19.2	34.5	49.6	64.5	79.2	93.4	120.7	144.9	167.4	187.3
36	6.6	14.7	19.3	34.6	49.8	64.8	79.5	93.8	121.2	145.6	168.3	188.5
38	6.6	14.7	19.3	34.7	49.9	65.0	79.8	94.2	121.8	146.4	169.3	189.8
40	6.7	14.7	19.4	34.8	50.1	65.3	80.2	94.6	122.4	147.2	170.3	191.1
42	6.7	14.8	19.4	34.9	50.3	65.6	80.5	95.1	122.9	148.0	171.3	192.3
44	6.7	14.8	19.5	35.0	50.5	65.8	80.8	95.5	123.5	148.7	172.3	193.6
46	6.7	14.8	19.5	35.2	50.7	66.1	81.2	95.9	124.1	149.5	173.3	194.8
48	6.7	14.9	19.6	35.3	50.9	66.3	81.5	96.3	124.7	150.3	174.3	196.0
50	6.7	14.9	19.6	35.4	51.1	66.6	81.8	96.7	125.2	151.0	175.2	197.2
52	6.7	14.9	19.7	35.5	51.3	66.8	82.2	97.1	125.8	151.8	176.1	198.3
54	6.7	15.0	19.7	35.6	51.4	67.1	82.5	97.5	126.3	152.5	177.0	199.5
56	6.8	15.0	19.8	35.7	51.6	67.3	82.8	97.8	126.8	153.2	177.9	200.6
58	6.8	15.0	19.8	35.8	51.8	67.6	83.1	98.2	127.4	153.8	178.8	201.6
60	6.8	15.0	19.9	36.0	51.9	67.8	83.4	98.6	127.8	154.5	179.6	202.6
62	6.8	15.1	19.9	36.1	52.1	68.0	83.6	98.9	128.3	155.1	180.4	203.6
64	6.8	15.1	20.0	36.2	52.3	68.2	83.9	99.2	128.8	155.7	181.2	204.6
66	6.8	15.1	20.0	36.3	52.4	68.4	84.2	99.6	129.3	156.3	182.0	205.5
68	6.8	15.2	20.1	36.3	52.6	68.6	84.4	99.9	129.7	156.9	182.7	206.5
70	6.8	15.2	20.1	36.4	52.7	68.8	84.7	100.2	130.1	157.5	183.4	207.4
72	6.8	15.2	20.1	36.5	52.8	69.0	84.9	100.5	130.6	158.1	184.1	208.2
74	6.9	15.2	20.2	36.6	53.0	69.2	85.2	100.8	131.0	158.6	184.8	209.1
76	6.9	15.3	20.2	36.7	53.1	69.4	85.4	101.1	131.4	159.1	185.5	209.9
78	6.9	15.3	20.3	36.8	53.3	69.6	85.7	101.4	131.8	159.7	186.2	210.7
80	6.9	15.3	20.3	36.9	53.4	69.8	85.9	101.7	132.2	160.2	186.8	211.5
82	6.9	15.3	20.3	37.0	53.5	69.9	86.1	101.9	132.6	160.7	187.4	212.3
84	6.9	15.3	20.4	37.0	53.6	70.1	86.3	102.2	132.9	161.2	188.0	213.0
86	6.9	15.4	20.4	37.1	53.8	70.3	86.5	102.5	133.3	161.7	188.7	213.8
88	6.9	15.4	20.4	37.2	53.9	70.5	86.8	102.8	133.7	162.2	189.2	214.5
90	6.9	15.4	20.5	37.2	54.0	70.5	86.9	102.9	133.9	162.4	189.5	214.8
92	6.9	15.4	20.5	37.3	54.0	70.6	86.9	103.0	134.0	162.5	189.7	215.0
94	6.9	15.4	20.5	37.3	54.0	70.6	87.0	103.0	134.0	162.6	189.9	215.3
96	6.9	15.4	20.5	37.3	54.1	70.7	87.1	103.1	134.2	162.8	190.1	215.5
98	6.9	15.4	20.5	37.3	54.1	70.7	87.1	103.2	134.3	162.9	190.2	215.7
100	6.9	15.4	20.5	37.3	54.1	70.7	87.2	103.2	134.3	163.0	190.3	215.7